Author(s): Koskinen, Jutta; Frimodig, Janne; Samulinen, Mikko; Tiihonen, Antti; Siljanto, Jimi; Haukka, Matti; Väisänen, Ari

Title: Optimization of Selective Hydrometallurgical Tantalum Recovery from E-Waste Using Zeolites

Year: 2024

Version: Published version

Please cite the original version:

Koskinen, J., Frimodig, J., Samulinen, M., Tiihonen, A., Siljanto, J., Haukka, M., & Väisänen, A. (2024). Optimization of Selective Hydrometallurgical Tantalum Recovery from E-Waste Using Zeolites. ACS Omega, Early online. https://doi.org/10.1021/acsomega.3c08907

ACS OMEGA

Open Access

http://pubs.acs.org/journal/acsodf

Article

Optimization of Selective Hydrometallurgical Tantalum Recovery from E-Waste Using Zeolites

Jutta Koskinen,* Janne Frimodig, Mikko Samulinen, Antti Tiihonen, Jimi Siljanto, Matti Haukka, and Ari Väisänen

Cite This: https://doi.org/10.1021/acsomega.3c08907

Read Online

ACCESS | Metrics & More | Article Recommendations | Supporting Information

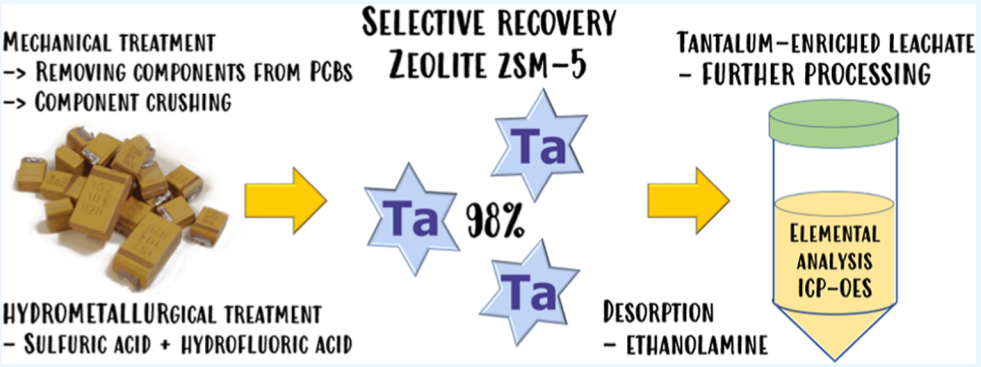

ABSTRACT: To protect future high-tech metal demand, a selective and efficient recovery method for tantalum from a tantalum-rich e-waste component sample was developed. Ultrasound-assisted digestion of the component sample was optimized, and the highest dissolution rate was achieved using a mixture of 8 mol/L H_2SO_4 and HF at a temperature of 60 °C. The determined amount of tantalum was as high as 11 000 ± 1000 mg/kg, which results in a high potential for recyclable tantalum. The other major elements of this complex e-waste fraction were silicon, iron, aluminum, and tin. Efficient recovery of tantalum from the leachate was performed using the zeolite material ZSM-5. Extremely high selectivity and a recovery rate of over 98% were obtained. In terms of adsorption efficiency, selectivity, and durability of the material, optimal adsorption was obtained using the diluted sample at 0.5 mol/L of H_2SO_4. The adsorption capacity of ZSM-5 for tantalum was determined to be 10.5 ± 0.6 mg/g, and tantalum was selectively eluted with 1:4 diluted ethanolamine with a yield of 87.2 ± 1.5%.

1. INTRODUCTION

In 2019, it was reported that 53.6 Mt of e-waste (electronic waste) was generated globally, of which only 9.3 Mt (17.4%) was officially documented for collection and recycling.[1] The fate of the undocumented e-waste stream, which accounts for 44.3 Mt (82.6%), is uncertain. However, it is assumed that most of the e-waste gets mixed with other waste streams due to the challenges of recycling and illegally transferred from first world countries to third world countries. The amount of generated e-waste is constantly increasing, with an annual growth rate of nearly 2 Mt between 2014 and 2019, while only 0.4 Mt is collected and recycled.

Printed circuit boards (PCBs) have been recognized as a valuable secondary raw material stream, particularly for the recycling of gold, copper, silver, and palladium, as its metal content is typically up to a hundred times higher than that of mined ores.[2,3] In addition to precious metals, valuable electronic components such as tantalum capacitors can be found on the surface of PCBs.[4] However, the focus in PCB recycling is primarily on recovering precious metals, and valuable metals like tantalum often end up in smelting slag and are thus discarded.[5] Increasing the collection rate and raising awareness among people are necessary actions to improve tantalum recycling, save resources, and prevent economic losses.[6]

Tantalum has been consistently included in the European Commission's list of critical raw materials (CRMs) for 7 consecutive years.[7] Tantalum mining in the EU was reportedly nonexistent in 2020, and consumption relied completely on imported goods.[8] However, the most recent report by World Mining Data cites a globally small, but still significant, yearly tantalum oxide production of approximately 15−20 t in Spain.[9] Tantalum is a significant raw material in terms of future high-

Received: November 9, 2023
Revised: February 20, 2024
Accepted: March 8, 2024

tech development, particularly in electronic components.[10] Capacitors are currently the most significant application of tantalum, and other notable uses include, e.g., superalloys, chemicals, and sputtering targets.[11]

According to the CRMs report, the total demand for tantalum has not been met at all through secondary streams by 2023.[7] However, research has already been conducted on the recycling and recovery of tantalum capacitors. Various methods have been explored to remove components from PCBs, including chemical dissolution,[12] manual and automated mechanical picking,[13] and laser integration into automated processes to melt component solders.[14−16] For the removal of the resin part of capacitors extracted from PCBs and the exposure of tantalum cores, mechanical treatment,[17] pyrolysis,[18−20] and supercritical water treatment[21] have been applied. In tantalum refining, various organic solvents such as MIBK (methyl isobutyl ketone) and TBP (tributyl phosphate) have been used, but the use of TSILs (task-specific ionic liquids) has been proposed as an environmentally friendly alternative.[22−24] Current studies involving tantalum recovery from e-waste using ion exchange resins or similar materials such as zeolites seem very scarce or close to nonexistent based on literature search. This publication aims to survey the new possibilities in this relatively uncharted field.

Zeolites are abundant naturally occurring adsorbent materials that are cost-effective and environmentally friendly.[25] The utilization of both natural and synthetic zeolites for purposes such as remediation of heavy metal-contaminated sites,[26] removal of heavy metals from wastewater,[27] and treatment of radioactive liquid waste[28] has been extensively studied. However, a focus on utilizing zeolites from a circular economy perspective is still lacking.

This study aimed to find a solution for the selective recovery of tantalum from the elementally complex e-waste fraction, namely, a component mixture leachate obtained by hydrometallurgical means using synthetic zeolites. The dissolution of the component sample was optimized with respect to sulfuric acid molarity with and without hydrogen fluoride (HF). Five zeolite materials were selected for the tests, which were screened using synthetic solutions. The most promising material, zeolite ZSM-5, underwent more specific adsorption, kinetics, capacity, and elution tests with a focus on tantalum.

2. MATERIALS AND METHODS

2.1. Samples. Synthetic sample solutions were prepared using PerkinElmer multielement standard solutions 2, 3, 4, and 5. More detailed information about the stock solutions is presented in Table S1. The component sample was obtained from a local electronics recycling center, where the components were mechanically removed from the PCBs of desktop computers, laptops, and set-top boxes. The component samples had been ground into fine powder with a particle size of <125 μm prior to receipt. No other physical pretreatments were performed to the sample, so it represents well the raw waste fraction coming from the recycling plant as is.

2.2. Materials and Reagents. Adsorbent materials zeolite ZSM-5, zeolite ferrierite, zeolite β, and zeolite Y were purchased from Thermo Scientific and molecular sieve 13X from Merck. More detailed information about adsorbents is presented in Table S2. Sulfuric acid (95−98% p.a.), nitric acid (65−69% p.a.), and hydrogen chloride (35−37% p.a.) from Honeywell were purchased from Fisher Scientific and HF (40%) from Merck. Ethylenediaminetetraacetic acid (EDTA, 99−101% p.a.), MIBK (≥99%), and ethanolamine (min 99%) were purchased from Sigma-Aldrich. All of the chemicals were used as received. High-purity water with a specific conductivity of 18.2 MΩ·cm was produced using Purelab Ultra by Elga.

2.3. Instrumentation. Elemental analyses were performed with a PerkinElmer Optima 8300 inductively coupled plasma-optical emission spectrometry (ICP-OES) instrument equipped with a GemCone Low-Flow nebulizer and a cyclonic spray chamber. The following parameters were used: sample flow rate of 1.5 mL/min, plasma gas flow of 8 L/min, nebulizer gas flow of 0.6 L/min, auxiliary gas flow of 0.2 L/min, and plasma power of 1500 W. The determinations of the element concentrations were performed using a five-point calibration (range 0−10 mg/L). More detailed measurement information is presented in the Supporting Information, in Table S3.

2.4. Dissolution of Tantalum-Rich E-Waste Fraction. Based on the literature, there are several potential methods for tantalum mineral decomposition, which include but are not limited to dissolution with sulfuric acid[29] or a combination of sulfuric acid with HF.[30] Therefore, the dissolution of the component sample was optimized in relation to the molarity of sulfuric acid with and without HF. The parameters presented in the study by Das and Ting[31] for the dissolution of e-waste with ultrasound assistance were used as applicable in the dissolution.

Experiments were carried out with sulfuric acid molarities of 0.1, 1, 2, 4, 6, 8, and 10 mol/L. 500 mg accurately weighed samples were leached with 10 mL of H_2SO_4 or with a mixture of 9 mL of H_2SO_4 and 1 mL of concentrated HF, using an ultrasonic bath and heated to 60 °C. The ultrasound-assisted dissolution was performed in 50 mL polypropylene centrifuge tubes in five cycles lasting 2 min each. Excess pressure was released from the centrifuge tubes between each cycle. The leached samples were quantitatively transferred and filtered (filter paper Whatman 41) into 50 mL volumetric flasks using high-purity water. Elemental concentrations of the sample solutions were determined, and the most effective digestion solution combination, 8 mol/L H_2SO_4 with HF, was selected.

Due to the heterogeneity of the sample, the dissolution was also performed using a sample weight of 2000 mg with 40 mL of optimal digestion solution. The determination of element concentration was performed more accurately when a larger sample weight was used.

2.5. Preliminary Adsorption Experiments. The adsorption performance screening of zeolite materials was done by using synthetic solutions with element concentrations of 1 mg/L in 0.5 mol/L of H_2SO_4. In batch tests, 10 mL of synthetic solution aliquots were mixed with 500 mg of adsorbent using magnetic stirring for 4 h at room temperature. After the adsorption period, centrifugation was performed to separate the phases of the solid−liquid mixtures. Elemental concentrations were determined from the solution phase before and after the zeolite treatment, and adsorption efficiencies for each adsorbate were calculated from the change in concentration using eq 1.

$$\text{adsorption efficiency (\%)} = \frac{c_i - c}{c_i} \times 100\% \quad (1)$$

where c_i is the concentration (mg/L) of the adsorbate before zeolite treatment and c is the concentration (mg/L) after treatment.

https://doi.org/10.1021/acsomega.3c08907
ACS Omega XXXX, XXX, XXX−XXX

2.6. Optimization of the Adsorption Process. Optimization of the adsorption process was performed in batch experiments. First, the most optimal sulfuric acid molarity for adsorption was determined. These tests were performed by using synthetic solutions as well as previously digested component samples. Acid molarities of 0.01, 0.1, 0.25, 0.5, 1.0, and 2.0 mol/L were adjusted to the solutions by dilution or addition, but the experimental setup remained otherwise identical compared to the preliminary adsorption tests. The determined pH values of the solutions are presented in the Supporting Information, in Table S4. Simultaneously, the durability of the zeolite material was evaluated in different sulfuric acid molarities based on the solubilities of silicon and aluminum, the main elements of the zeolite material.

The effect of adsorption time on adsorption efficiency was determined by mixing 25 mL of component leachate diluted to 0.5 mol/L with respect to acid with 200 mg of zeolite at room temperature. Sample aliquots of 0.5 mL were taken from the solution after 5, 15, 30, 45, 60, 90, 120, 180, and 240 min contact time and diluted appropriately for elemental analyses.

To elucidate the adsorption mechanism, the results from the adsorption time experiments were fitted to the commonly used pseudo-first-order (PFO) and pseudo-second-order (PSO) kinetic models. The linear fittings of PFO and PSO are shown in eqs 2 and 3, respectively.

$$\ln(Q_e - Q_t) = \ln(Q_e) - k_f t \tag{2}$$

$$\frac{t}{Q_t} = \frac{1}{k_s Q_e^{\,2}} + \frac{t}{Q_e} \tag{3}$$

where Q_e is equilibrium adsorption capacity (mg/g), Q_t is adsorption (mg/g) at time t (min), k_f is PFO's rate constant (1/min), and k_s is PSO's rate constant (g/mg·min).

The effect of the initial amount of adsorbate on the value of the adsorption capacity was investigated with the component leachate at 0.5 mol/L of H_2SO_4, using volumes of 10, 25, 50, 75, 100, and 125 mL. The test was performed at room temperature using 200 mg of zeolite and a contact time of 4 h. The experimental adsorption capacity values were determined by eq 4.

$$Q_e = \frac{(C_0 - C_e)\cdot V}{m} \tag{4}$$

where Q_e is equilibrium adsorption capacity (mg/g), C_0 and C_e are the initial and equilibrium adsorbate concentrations (mg/L), V is the volume of the solution (L), and m is the mass of adsorbent (g).

The experimental results of the adsorption capacity tests were fitted to the nonlinear models of Langmuir[32] and Freundlich[33] adsorption isotherms to elucidate the interaction between the adsorbate and adsorbent, eqs 5 and 6, respectively.

$$Q_e = \frac{Q_{max} b C_e}{1 + b C_e} \tag{5}$$

$$Q_e = K_F C_e^{\,1/n} \tag{6}$$

where Q_e is the equilibrium adsorption capacity (mg/g) and C_e equilibrium adsorbate concentrations (mg/L). Q_{max} expresses the theoretical maximum adsorption capacity (mg/g) and b represents the Langmuir constant (L/mg). n and K_F are the Freundlich constants, indicative of the adsorption intensity and adsorption capacity, respectively.

2.7. Desorption Experiments. Desorption was examined with batch tests for six different eluents, which were H_2SO_4, HNO_3, HCl, EDTA, MIBK, and ethanolamine. In the desorption experiments, zeolite batches from capacity determination tests were used, where the tantalum loadings were approximately 1.7−7.2 mg/g. Before the actual desorption experiments, the loaded ZSM-5 batches were treated three times with 20 mL of high-purity water using magnetic stirring and a 30 min contact time to prevent the possibly remaining leachate solution in the zeolite from causing errors in the desorption tests. Loaded and water-washed zeolite batches were contacted with 20 mL of eluent using a contact time of 4 h at room temperature. For mineral acids, stepwise elution was utilized. The loaded zeolite batches were first in contact with the most diluted mineral acids at 1 mol/L, after which the phases were separated. Next, the same zeolite batches were brought into contact with 3 mol/L acids and, after phase separations, with 6 mol/L acids. The EDTA eluent was used at 0.05 mol/L, whereas MIBK and ethanolamine were used undiluted.

The optimization of the desorption process was continued with ethanolamine by increasing the elution volumes to 30 and 40 mL, keeping the experimental setup otherwise unchanged. In the second test setup, ethanolamine was diluted with high-purity water in the ratio of 1:2, 1:4, and 1:8, while raising the elution temperature to 60 °C.

3. RESULTS AND DISCUSSION

3.1. Sample Elemental Composition. The elemental composition of the component sample according to the optimized dissolution is presented in Table 1. As can be seen, the sample is elementally very complex, creating a challenge from a recycling point of view. However, a significant 1.1 m % of tantalum makes this waste fraction an attractive secondary

Table 1. Elemental Composition of the Crushed and Digested E-Waste Component Sample (Mean ± s of 6 Replicates)

	component sample (mg/kg)
Si	61 000 ± 4000
Fe	31 000 ± 1100
Al	14 000 ± 2000
Sn	12 000 ± 1400
Ta	11 000 ± 1000
Ca	6900 ± 500
Mn	3000 ± 200
Nd	2600 ± 500
Zn	2500 ± 50
Ti	2100 ± 200
Ni	1400 ± 100
Mg	1000 ± 40
B	930 ± 30
Sb	730 ± 30
Cr	660 ± 30
Zr	510 ± 80
Pr	330 ± 50
Co	140 ± 40
Sm	140 ± 30
Sr	80 ± 20
Pb	77 ± 7
Cu	63 ± 7

https://doi.org/10.1021/acsomega.3c08907
ACS Omega XXXX, XXX, XXX−XXX

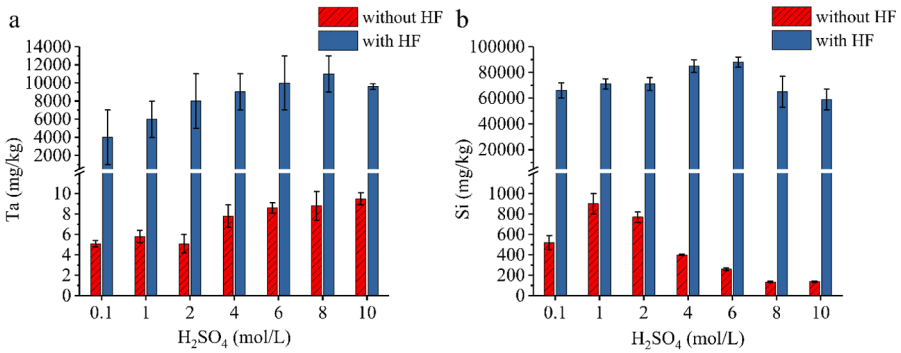

Figure 1. Effect of different H_2SO_4 molarities on the dissolution of the component sample for tantalum (a) and silicon (b) with and without HF.

stream, with the other major elements being silicon, iron, aluminum, and tin. The sample also contains valuable rare earth metals such as neodymium, praseodymium, and samarium.

3.2. Optimization of Sample Dissolution. The use of HF had a significant effect on the leachate's tantalum and silicon concentrations derived from elemental analyses of solutes. The amount of Ta, determined by dissolution without HF, was approximately 10 mg/kg. The presence of HF increases the solubility of tantalum by up to 1000 times. Without HF treatment, the amount of silicon was lower than 1000 mg/kg, but after treatment, it increased up to 50 000 mg/kg. Figure 1 shows the mean and standard deviations of the dissolution of three replicate samples for the concentrations of tantalum (Figure 1a) and silicon (Figure 1b). The heterogeneity of the sample fraction is manifested by large standard deviation values. The mixture of 8 mol/L H_2SO_4 with HF resulted in the most effective dissolution of tantalum, 11 000 ± 2000 mg/kg.

3.3. Preliminary Adsorption Experiments. Materials (zeolite ZSM-5, zeolite ferrierite, zeolite β, and zeolite Y) and molecular sieves were tested for the selective adsorption of tantalum from the synthetic solution. Molecular sieve 13X was dissolved in 0.5 mol/L H_2SO_4, and for practical reasons, it was rejected immediately from these experiments. The four other tested materials worked effectively, adsorbing tantalum more than 90% from the synthetic solution, where tantalum was present in its anionic form as nominal hexafluorotantalate, $[TaF_6]^-$. Figure 2 demonstrates the adsorption efficiency of the materials for the major elements of the component sample. Of these adsorbent materials, zeolite ZSM-5 was the most selective for tantalum, and its research was performed in more detail.

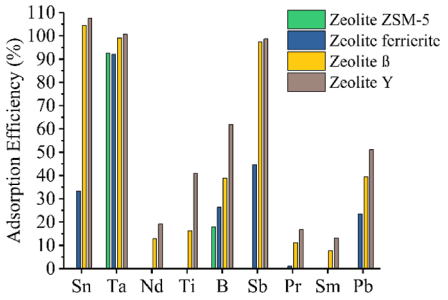

Figure 2. Adsorption efficiency of zeolite materials ZSM-5, ferrierite, β, and Y from synthetic 1 mg/L solutions in 0.5 mol/L H_2SO_4 for the selected elements.

Adsorption experiment results of tantalum without any kind of preliminary zeolite modifications were surprisingly good, as zeolites are known for their cation binding rather than anion binding properties, which are due to the natural negative charge of the zeolite body. Despite that, anions can also bind to the zeolite despite electrostatic repulsion. Zeolites with a higher Si/Al ratio show reduced ion exchange capacity but, on the other hand, better adsorption.[34] Results in the literature support the ability of the zeolite body to adsorb anions as well. For example, fluoride has been adsorbed with both natural[35] and modified zeolite.[36] Also, solutions for the removal of chloride[37] and phosphate[38] can be found in the adsorption studies of zeolites.

3.4. Optimization of the Adsorption Process. *3.4.1. Effect of Sulfuric Acid Molarity.* The effect of acid molarity on the adsorption efficiency of zeolite ZSM-5 was first tested with synthetic solutions. There was no significant difference in the adsorption efficiency of tantalum in the tested acid molarities, the results being between 90 and 95% regardless of the molarity of the acid background (Figure 3a). Only a small amount of boron is adsorbed to the material in all sulfuric acid molarities. Lead was partially removed from the solution only in the 2.0 mol/L H_2SO_4, indicating lead precipitation[39] rather than adsorption. Tests performed with the component leachate displayed even higher efficiencies for tantalum, resulting in a higher than 98% tantalum adsorption. Depending on the molarity of the acid, the material also adsorbed tin and antimony (Figure 3b).

Tin is present in the leachate sample at the same level as tantalum: 12 000 ± 1400 mg/kg (Sn) and 11 000 ± 1000 mg/kg (Ta). Compared to tantalum, the amount of antimony is lower by about 10-fold, at 730 ± 30 mg/kg. When aiming for the selective adsorption of tantalum, it is relevant to monitor the behavior of tin, which is present in the leachate sample in high concentration. The tests show that the adsorption should be carried out at 0.5−2.0 mol/L H_2SO_4, where tin is not readily adsorbed to the material.

ZSM-5 is proposed to adsorb size selectively, having pore diameters of ∼0.55 nm.[40] As shown in Figure 3a,b, tantalum is adsorbed from both the synthetic solution and the component leachate, where it is present as fluorocomplexes in both samples, nominally $[TaF_6]^-$. Additionally, from the synthetic solution, where HF is not present, antimony was not adsorbed to the ZSM-5 material. However, in the presence of excess HF in the component leachate, the adsorption of antimony was clearly enhanced, suggesting its conversion to a readily absorbed fluorocomplex of $[SbF_6]^-$ with a relatively similar size to $[TaF_6]^-$, having ionic diameters of ∼0.50 nm.[41] Due to

https://doi.org/10.1021/acsomega.3c08907
ACS Omega XXXX, XXX, XXX−XXX

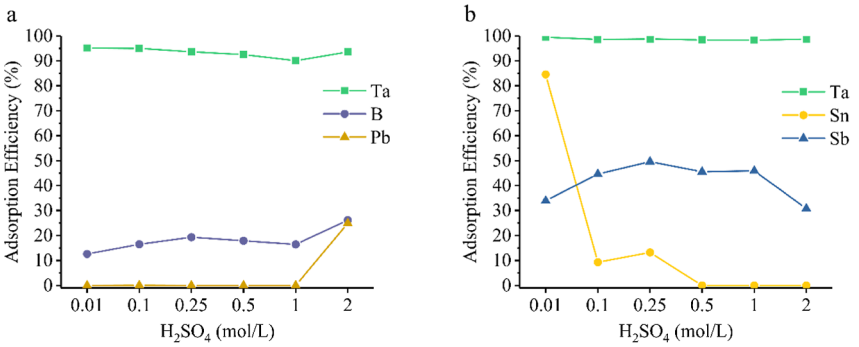

Figure 3. Adsorption efficiency of zeolite ZSM-5 for synthetic 1 mg/L solutions (a) and component leachate (b) at different sulfuric acid molarities for the major elements.

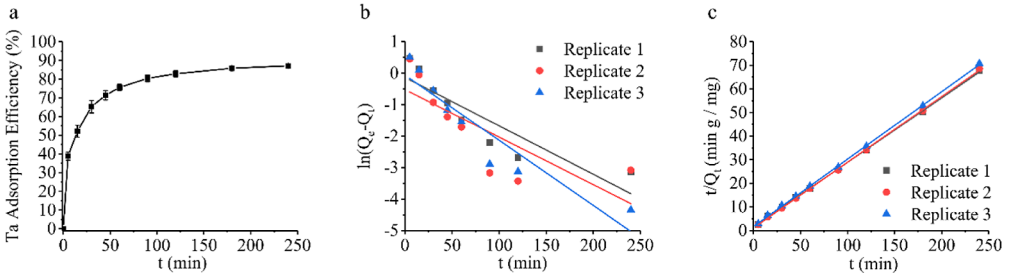

Figure 4. Adsorption efficiency of tantalum as a function of contact time, mean ± s of 3 replicates (a), PFO (b), and PSO (c) linear kinetics model fittings for the adsorption of tantalum.

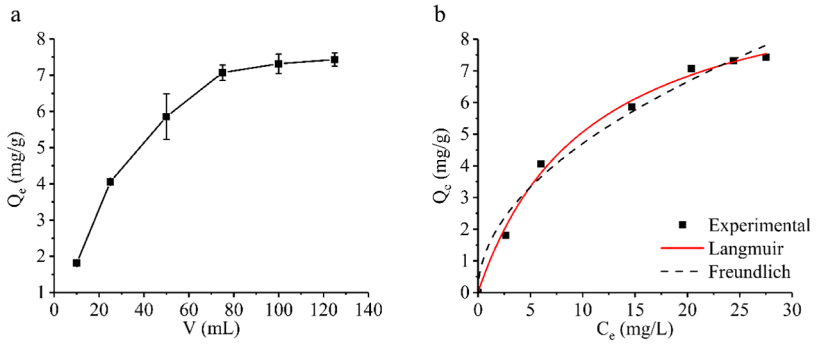

Figure 5. (a) Tantalum adsorption capacity versus sample solution volume for zeolite ZSM-5, mean ± s of 3 replicates. (b) Nonlinear models of Langmuir and Freundlich adsorption isotherms compared to the experimental results (mean of 3 replicates).

the similar ionic diameters and pore sizes, the most probable binding sites for roughly spherical fluorocomplexes are the pore openings on the surface of ZSM-5 material instead of the material's inner structures and the pore walls themselves. Also, due to hydration, the complexes pose an unreasonably tight fit to be able to bind deeper into the zeolite bulk.

The durability of the ZSM-5 material was examined during the adsorption tests performed on the component sample leachate. Due to the lack of an exact molecular formula of the zeolite material, the results are presented as changes in elemental concentrations present in the solutions (Table S5). During adsorption, the solubility of silicon is clearly greater than that of aluminum, which is explained by the material's SiO_2:Al_2O_3 molar ratio of 200−400:1 (Table S2). The more dilute the sulfuric acid is, the less stress the material experiences during adsorption.

When choosing the most optimal acid molarity for the adsorption, material wear and selectivity for tantalum must be considered. Based on the selectivity of the adsorption and the minimal stress on the material, 0.5 mol/L proved to be the optimal sulfuric acid molarity, which signified a dilution ratio of the component leachate of 0.347:1 for further experiments.

3.4.2. Effect of Adsorption Time. Figure 4a illustrates the effect of adsorption time on adsorption efficiency (%) in time intervals from 5 to 240 min. Already at 60 min, a significant adsorption of approximately 75% has been achieved. After that, increasing the contact time has only minor effect on the increase of adsorption efficiency. Adsorption equilibrium is finally established at about 180 min.

Figure 4b,c shows that the experimental data settle more precisely to the linear fitting of PSO (c) than the PFO (b) model. The calculated Q_e value of 3.582 mg/g of the PSO model is close to the experimental Q_e value of 3.513 mg/g, unlike the 0.7867 mg/g of the PFO model. Correlation coefficient (R^2) values for the fittings are 0.9997 (PSO) and 0.7827 (PFO). The exact parameter values are compiled separately in Table S6, where the rate constant values are also presented. A good correlation to the PSO model suggests that

https://doi.org/10.1021/acsomega.3c08907
ACS Omega XXXX, XXX, XXX−XXX

rate-limiting steps for adsorption involve ionic or covalent bonds associated with chemisorption.[42] The result also agrees with the reported literature, where zeolites are shown to be better fitted for the PSO model.[27]

3.4.3. Adsorption Capacity. Figure 5a illustrates the effect of the initial amount of tantalum on the value of the adsorption capacity. As the solution volume increases, the amount of tantalum in the solution increases from 0.4 to 5 mg. As Figure 5a shows, increasing the amount of tantalum no longer significantly increases the value of adsorption capacity, and the experimentally determined value of adsorption capacity settles to 7.4 ± 0.2 mg/g.

In the literature, there are studies on the utilization of zeolites, e.g., for the removal of anionic fluoride from drinking water, where a capacity of 0.47 mg/g has been determined for natural zeolite[35] and ∼2.3 mg/g for Fe(III) modified natural zeolite.[36] Modified zeolite has also been tested for wastewater treatment, which has shown a capacity of ∼1.8 mg/g for fluoride removal.[43] Compared to these results, the adsorption capacity of 7.4 ± 0.2 mg/g obtained for tantalum is significantly higher.

The adsorption isotherm nonlinear fittings of the capacity test average results are shown in Figure 5b, but linear fittings are also visible in Figure S1. By comparing the R^2 values of the Langmuir and Freundlich nonlinear models, which are 0.9941 and 0.9808, respectively, it can be observed that the experimental data fit the Langmuir model better. The exact parameter values are compiled separately for both fittings, nonlinear and linear, in Table S7, where the constant values are also presented. Based on the assumption of the Langmuir model, it can be stated that the interaction between tantalum and zeolite is probably limited to only one layer. The theoretical value of the maximum adsorption capacity according to the model can be calculated using the slope, which results in 10.5 ± 0.6 mg/g. Also, several studies dealing with zeolites support the suitability of the Langmuir isotherm in clarifying the interaction between adsorbate and adsorbent.[27]

3.5. Desorption Experiments. Among the tested eluents, ethanolamine was found to be the most effective and the only suitable eluent for tantalum. A recovery rate of 31 ± 3% was obtained for the tantalum desorption, as can be seen in Table S8. Antimony was adsorbed to the zeolite in small amounts and was not eluted with the tantalum. The results revealed a significant and noteworthy finding that only the small molecular base eluent appeared functional. Mineral acids and the larger molecular complexants, EDTA and MIBK, proved to be completely ineffective eluents in the experimental setups.

Increasing the volume of the ethanolamine eluent did not improve the desorption of tantalum from the zeolite (Table S9). In turn, raising the elution temperature to 60 °C together with a 1:4 dilution of the ethanolamine eluent increased the desorption to 87.2 ± 1.5%, as can be seen in Table S10. Dilution of ethanolamine lowers the viscosity of the eluent and improves contact with the loaded zeolite, but desorption requires the combined effect of dilution and heating. The same experiment performed at room temperature did not improve the desorption results.

Further research is required to convert tantalum from the eluent to a final product. The parallel studies[18,24] found in the literature regarding the recovery of tantalum support the possibility of producing good quality tantalum oxide. Utilizing the precipitation of tantalum from an aqueous solution of ethanolamine with added ammonium hydroxide and finishing the process with calcination to obtain tantalum oxide could be a viable route.

4. CONCLUSIONS

In this paper, an efficient and selective method for the recovery of tantalum from a complex e-waste component sample utilizing ultrasound-assisted digestion followed by adsorption with a commercial zeolite material ZSM-5 was developed. The adsorption of tantalum from the component leachate was performed with an extremely high recovery rate of over 98%.

The component sample obtained from a local electronics recycling center contained components removed from PCBs of desktop computers, laptops, and set-top boxes. Effective dissolution of tantalum, most likely originating from capacitors, can be performed only with a mixture of sulfuric acid and HF. The applied ultrasound-assisted digestion using a mixture of 8 mol/L H_2SO_4 in the presence of HF at a temperature of 60 °C was optimized. The concentration of tantalum determined by ICP-OES from the leachate was 11 000 ± 1000 mg/kg indicating a very high recovery potential.

For the adsorption experiments, diluted leachate with 0.5 mol/L H_2SO_4 was found to be optimal. In this concentration, only tantalum and antimony were adsorbed from the complex e-waste component leachate. Moreover, the concentrations of antimony were found to be 1000-fold lower than the tantalum concentrations in the loaded zeolite, resulting in a very low level of impurities. An adsorption capacity as high as 10.5 ± 0.6 mg/g was obtained for tantalum. Tantalum was selectively eluted from the material with 1:4 diluted ethanolamine with a yield of 87.2 ± 1.5%. This research shows a huge potential for tantalum recovery and recycling, despite the challenging sample fraction.

■ ASSOCIATED CONTENT

Supporting Information

The Supporting Information is available free of charge at https://pubs.acs.org/doi/10.1021/acsomega.3c08907.

Stock solutions' information; details of zeolite materials; ICP-OES measurement parameters; determined pH values of the samples; losses of the ZSM-5 due to dissolution; PFO and PSO parameters; Langmuir and Freundlich parameters; and desorption results of ZSM-5 (PDF)

■ AUTHOR INFORMATION

Corresponding Author

Jutta Koskinen − *Department of Chemistry, University of Jyväskylä, Jyväskylä FI-40014, Finland;* orcid.org/0009-0005-6514-7649; Email: jutta.m.koskinen@jyu.fi

Authors

Janne Frimodig − *Department of Chemistry, University of Jyväskylä, Jyväskylä FI-40014, Finland;* orcid.org/0000-0001-5280-0155

Mikko Samulinen − *Boliden Harjavalta, Harjavalta FI-29200, Finland*

Antti Tiihonen − *Department of Chemistry, University of Jyväskylä, Jyväskylä FI-40014, Finland;* orcid.org/0000-0001-8801-0710

Jimi Siljanto − *Department of Chemistry, University of Jyväskylä, Jyväskylä FI-40014, Finland*

https://doi.org/10.1021/acsomega.3c08907
ACS Omega XXXX, XXX, XXX−XXX

Matti Haukka − *Department of Chemistry, University of Jyväskylä, Jyväskylä FI-40014, Finland;* orcid.org/0000-0002-6744-7208

Ari Väisänen − *Department of Chemistry, University of Jyväskylä, Jyväskylä FI-40014, Finland*

Complete contact information is available at: https://pubs.acs.org/10.1021/acsomega.3c08907

Notes

The authors declare no competing financial interest.

■ ACKNOWLEDGMENTS

The authors would like to acknowledge the financial support and research facilities provided by the University of Jyväskylä.

■ REFERENCES

(1) Forti, V.; Baldé, C. P.; Kuehr, R.; Bel, G. The Global E-waste Monitor 2020: Quantities, flows, and the circular economy potential. United Nations University (UNU)/United Nations Institute for Training and Research (UNITAR) - co-hosted SCYCLE Programme, International Telecommunication Union (ITU) & International Solid Waste Association (ISWA), Bonn/Geneva/Rotterdam, https://collections.unu.edu/view/UNU:7737 (accessed May 23, 2023).

(2) Rao, M. D.; Singh, K. K.; Morrison, C. A.; Love, J. B. Challenges and opportunities in the recovery of gold from electronic waste. *RSC Adv.* **2020**, *10*, 4300−4309.

(3) Kaya, M. Recovery of Metals and Nonmetals from Electronic Waste by Physical and Chemical Recycling Processes. *Waste Manage.* **2016**, *57*, 64−90.

(4) Agrawal, M.; Singh, R.; Ranitović, M.; Kamberovic, Z.; Ekberg, C.; Singh, K. K. Global Market Trends of Tantalum and Recycling Methods from Waste Tantalum Capacitors: A Review. *Sustainable Mater. Technol.* **2021**, *29*, No. e00323.

(5) Bloodworth, A. Resources: Track Flows to Manage Technology-Metal Supply. *Nature* **2014**, *505* (7481), 19−20.

(6) Agrawal, M.; Jha, R.; Singh, R.; Singh, K. K. Flow and Stock Estimation of Tantalum for Sustainable Supply Chain. *Sustain. Prod. Consum.* **2022**, *34*, 385−394.

(7) European Commission. *Study on the Critical Raw Materials for the EU 2023 - Final Report*; European Commission, 2023.

(8) EU. European Union's Horizon 2020 research and innovation programme. Scrreen2 - Solutions for CRitical Raw Materials - a European Expert Network, Tantalum. 2023, https://scrreen.eu/wp-content/uploads/2023/12/SCRREEN2_factsheets_TANTALUM-update.pdf (accessed Feb 20, 2024).

(9) Reichl, C.; Schatz, M. *World Mining Data*; International Organizing Committee for the World mining Congresses, 2023; Vol. *38*, p 4.

(10) Zimmermann, T.; Gößling-Reisemann, S. Critical Materials and Dissipative Losses: A Screening Study. *Sci. Total Environ.* **2013**, *461*−*462*, 774−780.

(11) TIC. Bulletin No 172: Announcing the Anders Gustaf Ekeberg Tantalum Prize, in: Tantalum-Niobium International Study Center. 2018, https://www.tanb.org/images/T_I_C__Bulletin_no_172_(January_2018).pdf (accessed Apr 18, 2023).

(12) Bulach, W.; Schüler, D.; Sellin, G.; Elwert, T.; Schmid, D.; Goldmann, D.; Buchert, M.; Kammer, U. Electric Vehicle Recycling 2020: Key Component Power Electronics. *Waste Manag. Res.* **2018**, *36* (4), 311−320.

(13) Ramon, H.; Peeters, J. R.; Sterkens, W.; Duflou, J. R.; Kellens, K.; Dewulf, W. Techno-Economic Potential of Recycling Tantalum Containing Capacitors by Automated Selective Dismantling. *Procedia CIRP* **2020**, *90*, 421−425.

(14) Noll, R.; Ambrosch, R.; Bergmann, K.; Britten, S.; Brumm, H.; Chmielarz, A.; Connemann, S.; Eschen, M.; Frank, A.; Fricke-Begemann, C.; Gehlen, C.; Gorewoda, T.; Guolo, M.; Kurylak, W.; Makowe, J.; Sellin, G.; Siguier, M.; Tori, A.; Veglia, F. Next generation urban mining - Automated disassembly, separation and recovery of valuable materials from electronic equipment: overview of R&D approaches and first results of the European project ADIR *Proceedings of EMC*; ADIR, 2017.

(15) Noll, R.; Fricke-Begemann, C.; Connemann, S.; Meinhardt, C.; Sturm, V. LIBS Analyses for Industrial Applications - an Overview of Developments from 2014 to 2018. *J. Anal. At. Spectrom.* **2018**, *33* (6), 945−956.

(16) Noll, R.; Fricke-Begemann, C.; Schreckenberg, F. Laser-Induced Breakdown Spectroscopy as Enabling Key Methodology for Inverse Production of End-of-Life Electronics. *Spectrochim. Acta, Part B* **2021**, *181*, 106213.

(17) Agrawal, M.; Singh, R.; Singh, K. K. Recovery of Silica-Free Tantalum from Epoxy-Coated Tantalum Capacitors Using Hydrometallurgical Routes. *J. Environ. Chem. Eng.* **2022**, *10* (4), 108182.

(18) Chen, W. S.; Ho, H. J.; Lin, K. Y. Hydrometallurgical Process for Tantalum Recovery from Epoxy-Coated Solid Electrolyte Tantalum Capacitors. *Materials* **2019**, *12* (8), 1220.

(19) Niu, B.; Chen, Z.; Xu, Z. An Integrated and Environmental-Friendly Technology for Recovering Valuable Materials from Waste Tantalum Capacitors. *J. Cleaner Prod.* **2017**, *166*, 512−518.

(20) Chen, Z.; Niu, B.; Zhang, L.; Xu, Z. Vacuum Pyrolysis Characteristics and Parameter Optimization of Recycling Organic Materials from Waste Tantalum Capacitors. *J. Hazard. Mater.* **2018**, *342*, 192−200.

(21) Niu, B.; Chen, Z.; Xu, Z. Recovery of Tantalum from Waste Tantalum Capacitors by Supercritical Water Treatment. *ACS Sustain. Chem. Eng.* **2017**, *5*, 4421−4428.

(22) Micheau, C.; Arrachart, G.; Turgis, R.; Lejeune, M.; Draye, M.; Michel, S.; Legeai, S.; Pellet-Rostaing, S. Ionic Liquids as Extraction Media in a Two-Step Eco-Friendly Process for Selective Tantalum Recovery. *ACS Sustain. Chem. Eng.* **2020**, *8* (4), 1954−1963.

(23) Turgis, R.; Arrachart, G.; Michel, S.; Legeai, S.; Lejeune, M.; Draye, M.; Pellet-Rostaing, S. Ketone Functionalized Task Specific Ionic Liquids for Selective Tantalum Extraction. *Sep. Purif. Technol.* **2018**, *196*, 174−182.

(24) Micheau, C.; Lejeune, M.; Arrachart, G.; Draye, M.; Turgis, R.; Michel, S.; Legeai, S.; Pellet-Rostaing, S. Recovery of Tantalum from Synthetic Sulfuric Leach Solutions by Solvent Extraction with Phosphonate Functionalized Ionic Liquids. *Hydrometallurgy* **2019**, *189*, 105107.

(25) Han, B.; Weatherley, A. J.; Mumford, K.; Bolan, N.; He, J. Z.; Stevens, G. W.; Chen, D. Modification of Naturally Abundant Resources for Remediation of Potentially Toxic Elements: A Review. *J. Hazard. Mater.* **2022**, *421*, 126755.

(26) Belviso, C. Zeolite for Potential Toxic Metal Uptake from Contaminated Soil: A Brief Review. *Processes* **2020**, *8* (7), 820.

(27) Yuna, Z. Review of the Natural, Modified, and Synthetic Zeolites for Heavy Metals Removal from Wastewater. *Environ. Eng. Sci.* **2016**, *33* (7), 443−454.

(28) Jiménez-Reyes, M.; Almazán-Sánchez, P. T.; Solache-Ríos, M. Radioactive Waste Treatments by Using Zeolites. A Short Review. *J. Environ. Radioact.* **2021**, *233*, 106610.

(29) El-Hussaini, O. M.; Mahdy, M. A. Sulfuric Acid Leaching of Kab Amiri Niobium-Tantalum Bearing Minerals, Central Eastern Desert, Egypt. *Hydrometallurgy* **2002**, *64* (3), 219−229.

(30) Krismer, B.; Hoppe, A. Process for Recovering Niobium and/or Tantalum Compounds from Such Ores Further Containing Complexes of Uranium, Thorium, Titanium and/or Rare Earth Metals. U.S. Patent 4,446,116 A, 1984.

(31) Das, S.; Ting, Y. P. Evaluation of Wet Digestion Methods for Quantification of Metal Content in Electronic Scrap Material. *Resources* **2017**, *6* (4), 64.

(32) Langmuir, I. The Constitution and Fundamental Properties of Solids and Liquids. *J. Am. Chem. Soc.* **1916**, *38* (11), 2221−2295.

(33) Freundlich, H. Über Die Adsorption in Lösungen. *Z. Phys. Chem.* **1907**, *57U* (1), 385−470.

(34) Zagorodni, A. A. *Ion Exchange Materials: Properties and Applications*, 1st ed.; Elsevier, 2007.

(35) Gómez-Hortigüela, L.; Pérez-Pariente, J.; García, R.; Chebude, Y.; Díaz, I. Natural Zeolites from Ethiopia for Elimination of Fluoride from Drinking Water. *Sep. Purif. Technol.* **2013**, *120*, 224−229.
(36) Sun, Y.; Fang, Q.; Dong, J.; Cheng, X.; Xu, J. Removal of Fluoride from Drinking Water by Natural Stilbite Zeolite Modified with Fe(III). *Desalination* **2011**, *277* (1−3), 121−127.
(37) Osio-Norgaard, J.; Srubar, W. V. Zeolite Adsorption of Chloride from a Synthetic Alkali-Activated Cement Pore Solution. *Materials* **2019**, *12* (12), 2019.
(38) Ning, P.; Bart, H. J.; Li, B.; Lu, X.; Zhang, Y. Phosphate Removal from Wastewater by Model-La(III) Zeolite Adsorbents. *J. Environ. Sci.* **2008**, *20* (6), 670−674.
(39) Crockford, H. D.; Brawley, D. J. The Solubility of Lead Sulfate in Water and Aqueous Solutions of Sulfuric Acid1. *J. Am. Chem. Soc.* **1934**, *56* (12), 2600−2601.
(40) Song, W.; Justice, R. E.; Jones, C. A.; Grassian, V. H.; Larsen, S. C. Synthesis, Characterization, and Adsorption Properties of Nanocrystalline ZSM-5. *Langmuir* **2004**, *20*, 8301−8306.
(41) Roobottom, H. K.; Jenkins, H. D. B.; Passmore, J.; Glasser, L.; Glasser, L. Thermochemical Radii of Complex Ions. *J. Chem. Educ.* **1999**, *76* (11), 1570.
(42) Ho, Y. S.; McKay, G. Pseudo-Second Order Model for Sorption Processes. *Process Biochem.* **1999**, *34* (5), 451−465.
(43) Zhang, Z.; Tan, Y.; Zhong, M. Defluorination of Wastewater by Calcium Chloride Modified Natural Zeolite. *Desalination* **2011**, *276* (1−3), 246−252.

https://doi.org/10.1021/acsomega.3c08907
ACS Omega XXXX, XXX, XXX−XXX